ORIGINAL ARTICLE

Cancer Science WILEY

Systematic insight into the active constituents and mechanism of Guiqi Baizhu for the treatment of gastric cancer

Ling Li[1] | Xiao-jie Jin[1,2] | Jia-wei Li[1,3] | Cheng-hao Li[1] | Shuang-yan Zhou[4] |
Jun-jie Li[1] | Cai-qin Feng[5] | Dong-ling Liu[1,2] | Yong-qi Liu[1,6]

[1]Gansu University Key Laboratory for Molecular Medicine & Chinese Medicine Prevention and Treatment of Major Diseases, Gansu University of Chinese Medicine, Lanzhou, China

[2]College of Pharmacy, Gansu University of Chinese Medicine, Lanzhou, China

[3]School of basic medical sciences, Gansu University of Chinese Medicine, Lanzhou, China

[4]Chongqing Key Laboratory of Big Data for Bio Intelligence, Chongqing University of Posts and Telecommunications, Chongqing, China

[5]Affiliated Hospital of Gansu University of Chinese Medicine, Lanzhou, China

[6]Key Laboratory of Dun huang Medical and Transformation, Ministry of Education of The People's Republic of China, Gansu University of Chinese Medicine, Lanzhou, China

Correspondence
Jia-wei Li and Yong-qi Liu, Gansu University of Chinese Medicine, 35 Dingxi East Road, Cheng-guan District, Lanzhou, 730000, China.
Emails: Jiawei.Li@163.com; liuyongqi73@163.com

Funding information
Gansu University Key Laboratory for Molecular Medicine and Chinese Medicine Prevention and Treatment of Major Diseases, Gansu University of Chinese Medicine; National Natural Science

Abstract

Traditional Chinese medicine treatment of diseases has been recognized, but the material basis and mechanisms are not clear. In this study, target prediction of the anti-gastric cancer (GC) effect of Guiqi Baizhu (GQBZP) and the analysis of potential key compounds, key targets, and key pathways for the therapeutic effects against GC were carried out based on the method of network analysis and Kyoto Encyclopedia of Genes and Genomes enrichment. There were 33 proteins shared between GQBZP and GC, and 131 compounds of GQBZP had a high correlation with these proteins, indicating that the PI3K-AKT signaling pathway might play a key role in GC. From these studies, we selected human epidermal growth factor receptor 2 (HER2) and programmed cell death 1-ligand 1 (PD-L1) for docking; the results showed that 385 and 189 compounds had high docking scores with HER2 and PD-L1, respectively. Six compounds were selected for microscale thermophoresis (MST). Daidzein/quercetin and isorhamnetin/formononetin had the highest binding affinity for HER2 and PD-L1, with K_d values of 3.7 µmol/L and 490, 667, and 355 nmol/L, respectively. Molecular dynamics simulation studies based on the docking complex structures as the initial conformation yielded the binding free energy between daidzein/quercetin with HER2 and isorhamnetin/formononetin with PD-L1, calculated by molecular mechanics Poisson-Boltzmann surface area, of −26.55, −14.18, −19.41, and −11.86 kcal/mol, respectively, and were consistent with the MST results. In vitro experiments showed that quercetin, daidzein, and isorhamnetin had potential antiproliferative effects in MKN-45 cells. Enzyme activity assays showed that quercetin could inhibit the activity of HER2 with an IC_{50} of 570.07 nmol/L. Our study provides a systematic investigation

---

---

to explain the material basis and molecular mechanism of traditional Chinese medicine in treating diseases.

1 | INTRODUCTION

Gastric cancer is one of the most common malignant tumors in the world.[1] Due to the high heterogeneity of GC, it is a disease involving multiple genes and multiple targets, making treatment difficult.[2] Therefore, it is urgent to explore new treatment methods. Blockers targeting PD-L1,[3] PD-1,[4] HER2,[5] and other targets have become an important direction in study of GC. Overexpression of HER2 in GC patients is often positively correlated with PD-L1 expression, which could depend on the PI3K-AKT-mTOR pathway,[6] suggesting that the combination of drugs aimed at the above targets might be a new therapeutic pathway.

The multipoint fine adjustment, coordination, and efficacy enhancement effect of TCM have the characteristics of supporting the healthy factors and eliminating pathogenic factors, which should be advantageous in antitumor treatment. However, the current pharmacological evaluation method of TCM is still based on a single "disease gene-target drug" research model.[7] The specific mechanism for effects of many TCM formulas on cancer still needs further investigation, given that the chemical composition of TCM is very complex. The further evaluation of the pharmacodynamic function of TCM compounds and to determine their mechanisms of action are the focus of further research.

Guiqi Baizhu prescription is modified from Huang Qi prescription in volume 272 of "Prescriptions for Universal Relief".[8] Previous experiments showed that GQBZP could reduce liver[9] and kidney[10] functional damage induced by cisplatin, can improve the quality of life for patients with GC during chemotherapy, and regulate the immune balance.[11] However, the molecular mechanism and material basis of its effectiveness remain unclear.

Molecular docking and network pharmacology are widely used to study the material basis and mechanism of TCM in the prevention and treatment of disease.[12-14] Network pharmacology provides a new approach to systematically search for the active components and targets of TCM. Network pharmacology fits the multicomponent, multitarget dynamics of TCM and helps to identify the molecular mechanism of the overall effects of TCM.[15] Computer-aided drug design, such as molecular docking and molecular dynamics simulations, is used to calculate the interaction and affinity between a compound and a target to generate the material basis and mechanism of action of TCM by virtual screening.[16,17] For protein-ligand binding interactions, the MM-PBSA method is usually applied to the calculation of binding free energies (ΔG_{bind}) of small molecule ligands bound to large biomolecule receptors.[18] Microscale thermophoresis

is used to determine the affinity of the interacting biomolecules with high sensitivity.[19] Microscale thermophoresis can be used to identify appropriate compounds for cell experiments.

In this study, we identify key targets and potentially active compounds using network pharmacology, molecular docking, and MM-PBSA calculation. We used cell research, MST, and enzyme activity analysis to verify the activity of selected compounds and thereby identify and characterize the material basis and mechanism of GQBZP in the treatment of GC.

2 | MATERIAL AND METHODS

2.1 | Identification of GQBZP components and targets, PPI analysis, and KEGG enrichment

2.1.1 | Collection of compounds

The compounds of GQBZP were collected from Traditional Chinese Medicine Systems Pharmacology Database and Analysis Platform (TCMSP)[20] databases and were supplemented through searches of published reports. The structures of compounds were confirmed in PubChem databases.[21]

2.1.2 | Target analysis of the anti-GC effect of GQBZP

The simplified molecular input line entry specification (SMILES) code of each structure was obtained through PubChem. Swiss Target Prediction[22] was used to predict the potential targets of GQBZP. The drug targets for "GC" were retrieved by using "gastric cancer" and "gastric carcinoma" as keywords through TTD[23] and Drug Bank.[24] The common targets of GQBZP and GC were obtained by intersection.

2.1.3 | Analysis of the key compounds of GQBZP against GC

Based on the identified anti-GC targets of GQBZP, a herbs-compounds-targets network was constructed in Cytoscape 3.6.2,[25] and the degree value of compounds in the network was used to analyze the principal effective compounds of herbs.

2.1.4 | Kyoto Encyclopedia of Genes and Genomes enrichment and PPI analysis

The anti-GC targets of GQBZP were imported into DAVID.[26] The Select identifier was the official gene symbol, the List type was the gene list, the limited species was *Homo sapiens*, the threshold was *P* <.05, and KEGG pathway analysis was carried out. The online analysis platform Omicshare was used to visualize the enrichment path.[27] String[28] was used to analyze the PPI of the target, the species selected was *Homo sapiens*, and the comprehensive score for protein interaction was set as greater than 0.7 as the screening condition. Finally, the PPI information was imported into Cytoscape 3.6.2 for network analysis.

2.2 | Molecular docking

2.2.1 | Drug-like properties analysis of GQBZP

Through collection of compounds in GQBZP, a compound database of molecular docking was established. Drug-likeness was determined by Lipinski's rule.[29]

2.2.2 | Protein preparation

The 3D structure of HER2 (PDB ID: 3RCD)[30] and PD-L1(PDB ID: 4Z18)[31] were downloaded from PDB databases.[32] The binding pocket of HER2 was the substrate-binding site and the active residues of HER2 were Lys753, Asp863, Thr862, Phe864, and Met801.[30] The PD-L1 binding pocket belonged to protein-protein interface binding sites and the potential active residues were Tyr56, Met115, Ala121, Tyr123, and Asp122.[31] Finally, the Prep Wiz module was used to preprocess these targets in Schrödinger. The screen greedy box center read of HER2 was x cent −38.142190, y cent −29.102648, and z cent −74.036287, with the size of the box at 10 Å. The screen greedy box center read of PD-L1 was x cent −6.006301, y cent −15.078195, and z cent −4.842327, with the size of the box at 10 Å.

2.2.3 | Molecular docking

Compounds collected were prepared by the LigPrep module.[32] Molecular docking was carried out using the Glide module with the extra docking precision method (Glide XP) in Schrödinger 2020-2.[34,35] The corresponding low-energy conformation was obtained by the molecular mechanics force fields. Finally, Epik 28[36] used a pH value of 7.0 ± 2.0 to conditionally allocate the ionization state and undertake docking calculations. The interaction mechanism between drug components and protein was studied by Pymol.[37]

2.3 | Microscale thermophoresis assay

The TCM compounds' affinity for proteins was measured by MST Reagent (NanoTemper Technologies) and Monolith NT.115 (NanoTemper Technologies). The proteins (Human PD-L1 Fc Protein, PeproTech; and Recombinant Human Her2/ErbB2 Protein, Sino Biological) were desalted into MST buffer (10 mmol/L HEPES, pH 7.5, 150 mmol/L NaCl) before the experiment. The proteins were fluorescently labelled and the protein concentration was adjusted to 10 μmol/L. Fluorescent dye NT-647-NHS was added, mixed, and incubated for 30 min at 25°C in the dark. For each assay, the labelled protein (approximately 0.1 μmol/L) was mixed with the same volume of unlabeled ligands quercetin (Sigma-Aldrich), daidzein (Sigma-Aldrich), isorhamnetin (Sigma-Aldrich), or formononetin (Saitong) in 16 serial concentrations at room temperature. The samples were then loaded into premium capillaries and measured at 25°C by using 20% Light Emitting Diode power and medium MST power. Data analyses were undertaken using MO Affinity Analysis 2.2.4 software. With a confidence of 68%, the K_d value is within the given range.

2.4 | Molecular dynamics

2.4.1 | System setup

The initial structure of the proteins complex with compounds was obtained from molecular docking. Structure optimization and frequency calculations for the small molecule quercetin, daidzein, isorhamnetin, and formononetin were determined at the HF/6-31G* level of Gaussian 09. The restrained electrostatic potential was used to describe the partial atomic charges. The parameters for the small molecules were generated from Amber force field.[38] The standard Amber force field for bioorganic systems[39] was used to describe the protein. The counter ions were added to neutralize each system. All systems were solvated using an atomistic TIP3P[39] water box with at least 10 Å distance around the complex.

2.4.2 | Molecular dynamics simulations

Amber20[40] was used throughout the simulation process and the force field FF14SB was selected to describe the protein. The energy minimization was first carried out with the steepest descent method and switched to conjugate gradient every 2500 steps for 5000 steps with a 0.1 kcal/mol·Å^2 restraint on all atoms of the complexes. Following this step, another two rounds of energy minimization were undertaken by restraining only protein and further releasing all the restraints for 5000 steps of each round. Long-range Coulombic interactions were handled using the particle mesh Ewald (PME) summation.[39] For the equilibration and subsequent production runs, the SHAKE algorithm[41] was used on all atoms covalently bonded to a hydrogen atom, allowing for an integration time step of 2 fs. The

systems were gently annealed from 0 to 310 K over a period of 50 ps using a Langevin thermostat with a coupling coefficient of 1.0/ps and a force constant 2.0 kcal/mol·Å² on the complex. All subsequent stages were carried out in the isothermal isobaric (NPT) ensemble using a Berendsen barostat with a target pressure of 1 bar. An additional five rounds of MD (100 ps each at 310 K) were carried out with decreasing restraint weights from 2.0, 1.5, 1.0, 0.5 to 0.1 kcal/mol·Å². By releasing all the restrains, the system was again equilibrated for 500 ps. The production phase of the simulations was run without any restrains for a total of 50 ns.

2.4.3 | Binding free energy calculations

The MM-PBSA calculation was carried out using Amber20.[42] The first step of the MM-PBSA method is the generation of multiple snapshots from a molecular dynamics trajectory of the protein-ligand complex, which was stripped of water molecules and counter ions. Two hundred and fifty snapshots, equally spaced at 20 ps intervals, were extracted from the equilibration section (last 10 ns) of the molecular dynamics trajectory. For each snapshot, the free energy was calculated for each molecular species (complex, protein, and ligand). The binding free energy was computed as the difference[42]:

$$\Delta G_{bind} = G_{complex} - G_{protein} - G_{ligand}$$

2.5 | Enzyme activity assays of HER2

All enzymatic reactions were carried out at 30°C for 40 min. The 50 μl reaction mixture contained 40 mmol/L Tris, 10 mmol/L MgCl₂, 0.1 mg/ml BSA, 1 mmol/L DTT, 10 μmol/L ATP, 0.4 ng/μl HER2 kinase, and 100 μmol/L lipid substrate. The compounds were diluted in 10% DMSO and 5 μl of the dilution was added to a 50 μl reaction; the final concentration of DMSO was 1% in all reactions. These assays were undertaken using the HTRF kinEASE TK kit (Cisbio). The fluorescent signals were correlated with the amount of ATP present and were inversely correlated with kinase activity. The IC_{50} values were calculated using nonlinear regression with normalized dose-response fit.

2.6 | Screening, culture, and cytotoxicity detection of GC cells

Human GC MKN-45, SGC-7901, and BGC-823 cell lines and the human gastric mucosal epithelial GES-1 cell line were cultured in DMEM (Hyclone) with 10% FBS, 1% penicillin, and 1% streptomycin, incubated in 5% CO₂.

Protein (50 μg) from the MKN-45, SGC-7901, BGC-823, and GES-1 cell lines was harvested from RIPA lysis buffer and separated by 10% SDS-PAGE. Protein was transferred to a PVDF membrane (Millipore). After blocking with 10% nonfat milk, membranes were incubated with primary Abs for PD-L1 (GeneTex) or HER2 (Abcam).

Membranes were incubated with secondary Abs followed by enhanced chemiluminescence reagents (Yeasen). The GAPDH protein was used as a reference.[43] The GC cells were incubated with HER2 Ab (1:250) or PD-L1 (1:200) diluted in PBS containing 1% BSA and incubated overnight at 4°C, followed by addition of fluorescent-labeled secondary Abs (Alexa Fluor 647; Abcam) for 1 h at room temperature.[44]

MKN-45 cells with approximately 6×10^3 cells/well were plated in a 96-well standard microplate in DMEM with 10% FBS, 1% penicillin, and 1% streptomycin, and incubated in 5% CO₂. After the cells became adherent, the medium was replaced and different doses of compounds were added. Cells were exposed to various concentrations (five serial dilutions in triplicate) of quercetin, daidzein, isorhamnetin, and formononetin. After 72 h of culture, the medium was removed and 100 μl DMEM, supplemented with 10% CCK-8, was added to each well and incubated in the dark for an additional 2 h at 37°C. The absorbance was then measured using microplate reader (iMark; Bio-Rad) at a wavelength of 450 nm. The cell viability was expressed as a percentage of the control values (blank). The experiments were done in triplicate.

2.7 | Statistical analysis

Differences among three or more experimental samples were analyzed by ANOVA. Significance was set at $P < .05$.

3 | RESULTS

3.1 | Identification of GQBZP components and targets, PPI analysis, and KEGG enrichment

The seven herbs in GQBZP all belong to the spleen meridian, which has the characteristics of both attacking and supplementing by strengthening the spleen and stimulating blood flow. Information on each herb is shown in Table 1. In this study, 787 compounds were collected, which were mainly flavonoids, alkaloids, and coumarins. Their structures are shown in Figures S1-S61.

The potential targets of the seven herbs of GQBZP were predicted by the Swiss Target Prediction database, and 885 targets were obtained after removing duplicates. One hundred and twenty nine GC potential targets were obtained from the Drug Bank and TTD database after removing duplicates, and 33 key potential targets were finally obtained after intersection. The herb-compound-target network consists of 171 nodes and 938 edges (Figure 1A), with green, blue, and purple representing herbs, compounds, and key targets, respectively. The top 10 compounds are kaempferol, naringenin, jaranol, mairin, quercetin, isorhamnetin, (3S,8S,9S,10R,13R,14S,17R)-10,13-dimethyl-17-[(2R,5S)-5-propan-2-yloctan-2-yl]-2,3,4,7,8,9,11,12,14,15,16,17-dodecahydro-1H-cyclopenta[a]phenanthren-3-ol, sitosterol, beta-sitosterol, and 1,3-dihydroxy-8,9-dimethoxy-6-benzofurano[3,2-c] chromenone. HSP90AA1 (66), EGFR (66), KDR (62), PTGS1 (62), SRC (61), CA9 (52),

TABLE 1 Composition and characteristics of each constituent of Guiqi Baizhu prescription

| Drug name/English name	Medicinal part	Channel tropism	Medicinal efficacies	Role in the prescription
Astragali radix	Root, rhizome	Lung, spleen	Invigorate the Zhong qi, detoxification, purulence, diuresis	Monarch
Atractylodis macrocephalae	Root, rhizome	Spleen, lung, spleen	Tonify spleen and replenish qi	Monarch
Angelicae	Rhizome	Heart, spleen, liver	Replenish blood and activate blood	Minister
Paeoniae radix alba	Root	Spleen, liver	Nourish blood and relieve pain	Minister
Pericarpium citri reticulatae	Mature pericarp	Spleen, lung	Regulate qi, invigorate spleen, and dry dampness	Assistant
Rhubarb	Root, rhizome	Spleen, stomach, large intestine, liver, pericardium	Promote the excretion of toxins and evil, regulate qi and stagnation, invigorate the spleen and stomach, and activate qi to promote blood circulation	Assistant
Glycyrrhizae	Root, Rhizome	Heart, spleen, lung, spleen	Invigorate spleen and replenish qi, pain relief, and harmonize various medicines	Messenger
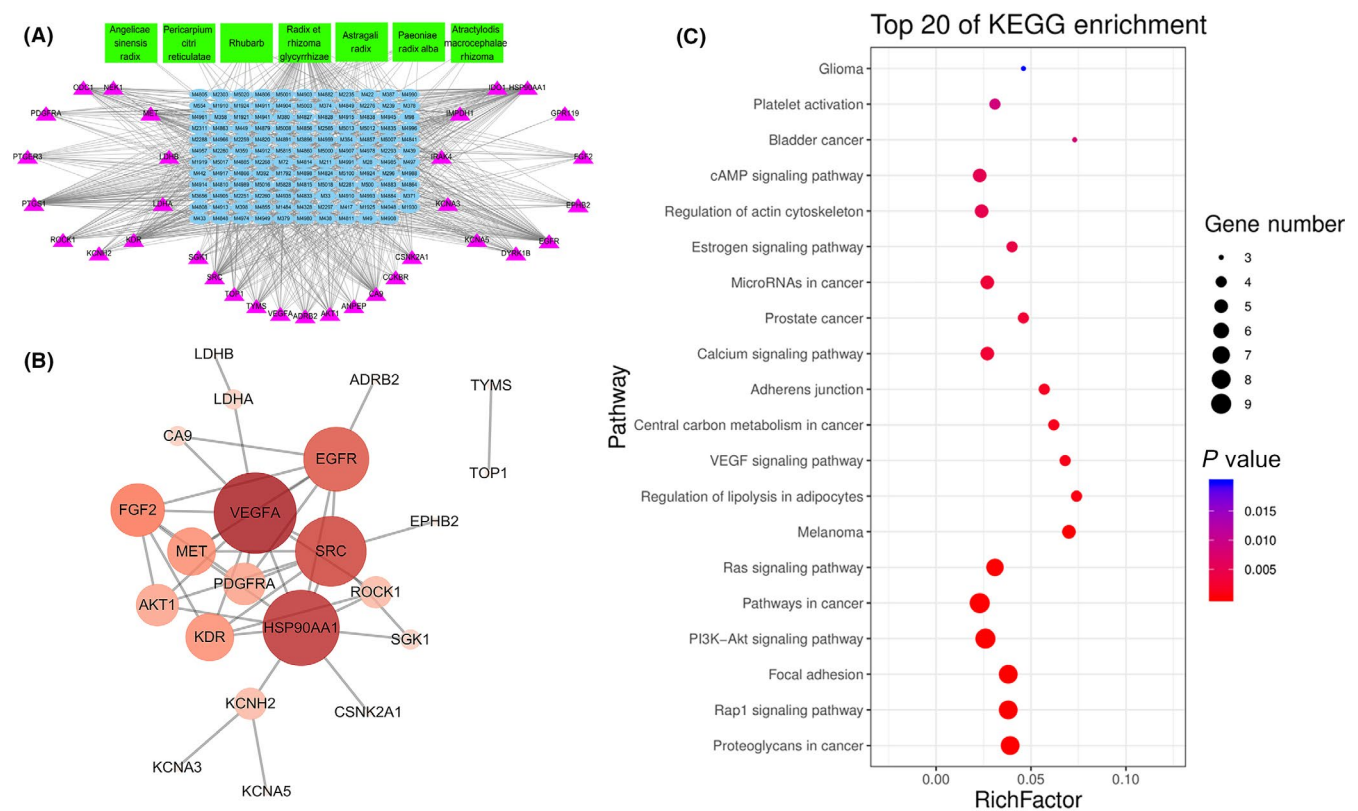
FIGURE 1 Identification of Guiqi Baizhu prescription (GQBZP) components and targets, protein-protein interaction (PPI) analysis, and Kyoto Encyclopedia of Genes and Genomes (KEGG) enrichment. A, Traditional Chinese medicine-compound-target network of GQBZP. B, PPI network of targets of GQBZP. C, KEGG analysis of potential targets. The bubble size represents the number of genes enriched in this pathway, the bubble color difference represents the level of gene enrichment in this pathway, and the circle size represents the number of targets contained in the pathway. The redder the color, the smaller the P value. VEGF, vascular endothelial growth factor

MET (48), TOP1 (37), ODC1 (34), and AKT1 (29) are the potential key targets of GQBZP (Table 2). The PPI network (Figure 1B) was constructed with highly reliable (more than 0.7) targets of interaction, which includes 22 nodes and 41 edges; in the network, circles represent targets, and the darker the color and bigger the size, the greater the degree value. In the protein interaction network of GQBZP, VEGFA (11), HSP90AA1 (10), SRC (9), EGFR (8), and FGF2 (6) are the top five nodes, which could play important roles in the treatment process.

The potential protein targets could play an important role in GC, but whether they are a drug target and can be targeted for

TABLE 2 Key targets of Guiqi Baizhu prescription in the treatment of gastric cancer

No.	Gene name	Uniprot ID	Protein name
1	HSP90AA1	P07900	Heat shock protein 90 alpha family class A member 1
2	EGFR	P00533	Epidermal growth factor receptor
3	KDR	P35968	Vascular endothelial growth factor receptor 2
4	PTGS1	P23219	Cyclooxygenase-1
5	SRC	P12931	Tyrosine-protein kinase SRC
6	CA9	Q16790	Carbonic anhydrase IX
7	MET	P08581	Hepatocyte growth factor receptor
8	TOP1	P11387	DNA topoisomerase I
9	ODC1	P11926	Ornithine decarboxylase
10	AKT1	P31749	Serine/threonine-protein kinase AKT

drug development still requires practical detection. Among the HER family, HER2 appears as a keystone for ERBB signaling and is a key feature for cross-talk between numerous cell signaling pathways.[45] Both EGFR and HER2 are closely related to the abnormal proliferation of tumor cells, and the abnormal expression of HER2 in tumor tissues promotes the proliferation of tumor cells.[46] At present, there are many studies on EGFR/HER2 dimers, and trastuzumab targeting HER2 has been approved for clinical treatment of GC. Therefore, HER2 was selected as the key target of molecular docking.

The enrichment of the KEGG pathway of GQBZP in the treatment of GC is shown in Figure 1C. The result showed that the PI3K-AKT signaling pathway might play a role in the treatment of GC using GQBZP. Overexpression of HER2 in GC patients is often positively correlated with PD-L1 expression, which could depend on the PI3K-AKT-mTOR pathway,[6] suggesting that the combination of drugs aimed at the above targets could be a promising treatment strategy. Suh et al[47] reported that PD-L1 expression is positively correlated with EGFR/HER2 signaling pathway activation in seven GC cell lines. Targeted multichannel combination therapy can further improve the immune response and survival rate, including the combination of targeted therapy, chemotherapy, and antiangiogenic therapy.[48] Therefore, we believe that PD-L1 overexpression is related to the EGFR/HER2 pathway, and drugs targeting these pathways could reduce the inhibition of antitumor immunity. According to a report released by the Cancer Research Institute,[49] there were 1176 combined therapy studies in 2018, of which 21 were PD-1/PD-L1 inhibitors combined with HER2. Therefore, based on the results of network pharmacology, our previous study, and other published reports, HER2 and PD-L1 were selected as therapeutic targets to explore the effect and possible molecular mechanisms of multitarget combination therapy for GC.

3.2 | Molecular docking

In this study, 787 compounds were collected, 483 of which conformed to Lipinski's rule (Table 3). The structure of HER2 and PD-L1 proteins are shown in Figure 2.

After docking, scores were obtained and expressed in absolute values, and the small molecules with high scores in different herbs are shown in Table 3. The results show that 385 compounds having drug-like properties in GQBZP had a docking score of −4 or lower with HER2, and 189 had a docking score of −4 or lower with PD-L1. Table 4 and Table 5 list the small molecules with higher scores after docking with the target proteins. The docking results show that *Astragali radix*, Angelicae, and rhubarb in GQBZP contained potential active ingredients, which corresponds with the effects of *Astragali radix* in prescriptions on invigorating qi and the spleen, Angelicae in nourishing blood and replenishing blood, and rhubarb in promoting blood circulation. From the two-way effect of regulating immunity and treating tumors, it preliminarily explains that GQBZP might play a coordinated role in the treatment of GC through multiple targets, such as HER2 and PD-L1.[50]

3.3 | Microscale thermophoresis analysis and molecular dynamics

Six compounds that targeted HER2 and PD-L1 were selected for MST experiments after docking. More than 12 concentration gradients were used to fit the K_d value of the equilibrium dissociation constant (Figure 3). Daidzein/quercetin and isorhamnetin/formononetin had the highest binding affinity for HER2 and PD-L1, with K_d values of 3.7 μmol/L and 490, 667, 355 nmol/L, respectively, indicating a strong potential targeting ability.

To further study the interaction pattern of the above four compounds at the molecular level, MD of the corresponding complexes was carried out. As shown in Figure 4, for HER2, during a 50 ns MD the interaction modes were stable, as indicated by comparing the initial and final structures of the protein-ligand complex, and the interaction between binding pocket residues was relatively conservative.[51,52] The interactive residues were Met801, Lys753, and Asp863, and hydrogen bonding was the main interaction (Figure 4A-D). In the process of binding, the interactive amino acids of the binding pocket with small molecules required conformational adjustment of the molecules rather than the protein. For example, quercetin (Figure 4A,B) and daidzein (Figure 4C,D) added new hydrogen bonding with Gln799 and Cys805, respectively.

For PD-L1, during a 50 ns MD, the interaction mode of isorhamnetin and PD-L1 was stable and isorhamnetin interacted with Glu58 through hydrogen bonding (Figure 4E,F). The binding conformation of formononetin with PD-L1 changed after MD (Figure 4G,H). The binding pocket of PD-L1 is located in a plane composed of β-sheets, which means that the structure is inflexible and the amino acids in the binding pocket cannot adjust in the binding of small molecules. Thus, a conformational adjustment of small molecules to better adapt to the

	Compounds	Drug-like properties	Docking with HER2	Docking with PD-L1
Astragali radix	87	37	33	19
Atractylodis macrocephalae	55	36	29	10
Angelicae	125	89	69	25
Paeoniae radix alba	85	40	28	8
Pericarpium citri reticulatae	63	51	26	5
Rhubarb	92	44	37	17
Glycyrrhizae	280	186	163	95
Total	787	483	385	189

TABLE 3 Number of Guiqi Baizhu prescription compounds before and after drug-like identification and after docking with human epidermal growth factor receptor 2 (HER2)/programmed cell death 1-ligand 1 (PD-L1) protein (≤−4)
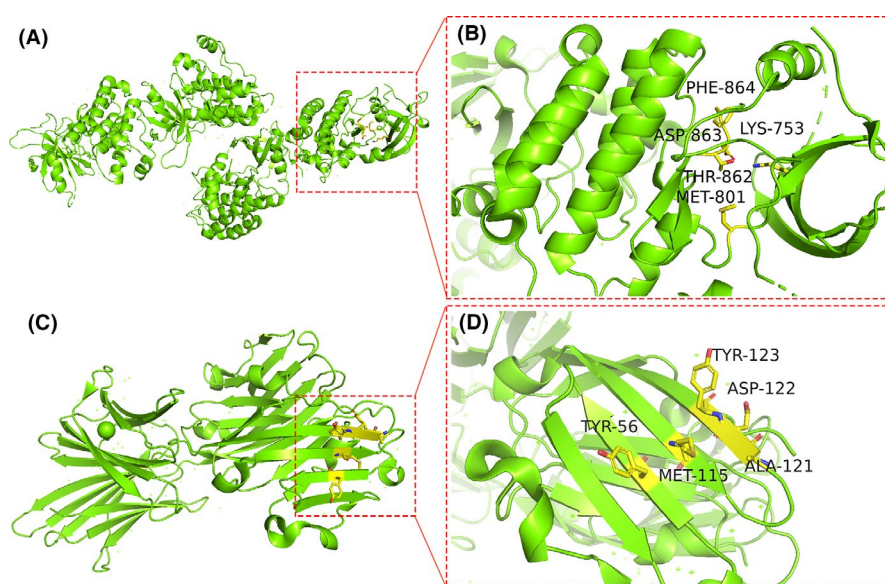

FIGURE 2 Crystal structure and amino acid sites of target proteins. A, Structure of human epidermal growth factor receptor 2 (HER2). B, Amino acid sites of HER2. C, Structure of programmed cell death 1-ligand 1 (PD-L1). D, Amino acid sites of PD-L1

TABLE 4 Compounds with higher scores for docking with human epidermal growth factor receptor 2 in Guiqi Baizhu prescription

TCMSP ID	TCM drug	Compound name	Docking score	MW	HBA	HBD	logpo/W	Rotor
MOL000030	*Atractylodis macrocephalae*	Acridine	−9.743	148.204	1.70	1	2.870	3
MOL000038	*Atractylodis macrocephalae*	Akridin	−9.181	179.221	1.00	0	3.403	0
MOL000040	*Atractylodis macrocephalae/ Angelicae/Glycyrrhizae*	Scopoletol	−8.488	192.171	4.00	1	1.021	2
MOL000044	*Atractylodis macrocephalae*	Atractylenolide II	−7.960	232.322	3.00	0	2.666	0
MOL000098	*Astragali radix/Glycyrrhizae*	Quercetin	−7.788	302.240	5.25	4	0.472	5
MOL000106	Paeoniae radix alba	Pyrogallol	−7.780	126.112	2.25	3	0.103	3
MOL000354	*Astragali radix/Glycyrrhizae*	Isorhamnetin	−7.533	316.267	5.25	3	1.402	5
MOL000259	Pericarpium citri reticulatae/ Angelicae	Carvacrol	−7.583	150.220	0.75	1	3.291	2
MOL000390	*Astragali radix*	Daidzein	−7.331	254.242	4.00	2	1.845	3
MOL000396	*Astragali radix*	(+)− Syringaresinol	−7.275	418.443	7.90	2	3.387	6

HBA, hydrogen bond acceptors; HBD, hydrogen bond donors; MW,molecular weight; logPo/w, lipid-water partition coefficient; Rotor,number of rotatable bonds; TCM, traditional Chinese medicine; TCMSP, Traditional Chinese Medicine Systems Pharmacology Database and Analysis Platform.

TABLE 5 Compounds with higher scores for docking with programmed cell death 1-ligand 1 in GQBZP

TCMSP ID	TCM drug	Compound name	Docking score	MW	HBA	HBD	logPo/w	Rotor
MOL000030	*Atractylodis macrocephalae*	Acridine	−5.575	148.204	1.70	1	2.870	3
MOL000040	*Atractylodis macrocephalae/ Angelicae/Glycyrrhizae*	Scopoletol	−5.417	192.171	4.00	1	1.021	2
MOL000098	*Astragali radix/Glycyrrhizae*	Quercetin	−5.215	302.240	5.25	4	0.472	5
MOL000106	*Paeoniae radix alba*	Pyrogallol	−5.217	126.112	2.25	3	0.103	3
MOL000114	*Astragali radix*	Vanillic acid	−5.198	168.149	3.50	2	1.042	3
MOL000354	*Astragali radix/Glycyrrhizae*	Isorhamnetin	−4.998	316.267	5.25	3	1.402	5
MOL000389	*Astragali radix/Atractylodis macrocephalae*	Ferulic acid (CIS)	−4.96	194.187	3.5	2	1.586	5
MOL000392	*Astragali radix/ Glycyrrhizae*	Formononetin	−4.883	268.268	4.0	1	2.698	3
MOL000414	*Astragali radix*	Caffeic acid	−4.876	180.160	3.5	3	0.636	5
MOL000416	*Astragali radix*	Lariciresinol	−4.865	360.406	6.4	3	2.916	8

HBA, hydrogen bond acceptors; HBD, hydrogen bond donors; MW, molecular weight; logPo/w, lipid-water partition coefficient; Rotor, number of rotatable bonds; TCM, traditional Chinese medicine; TCMSP, Traditional Chinese Medicine Systems Pharmacology Database and Analysis Platform.
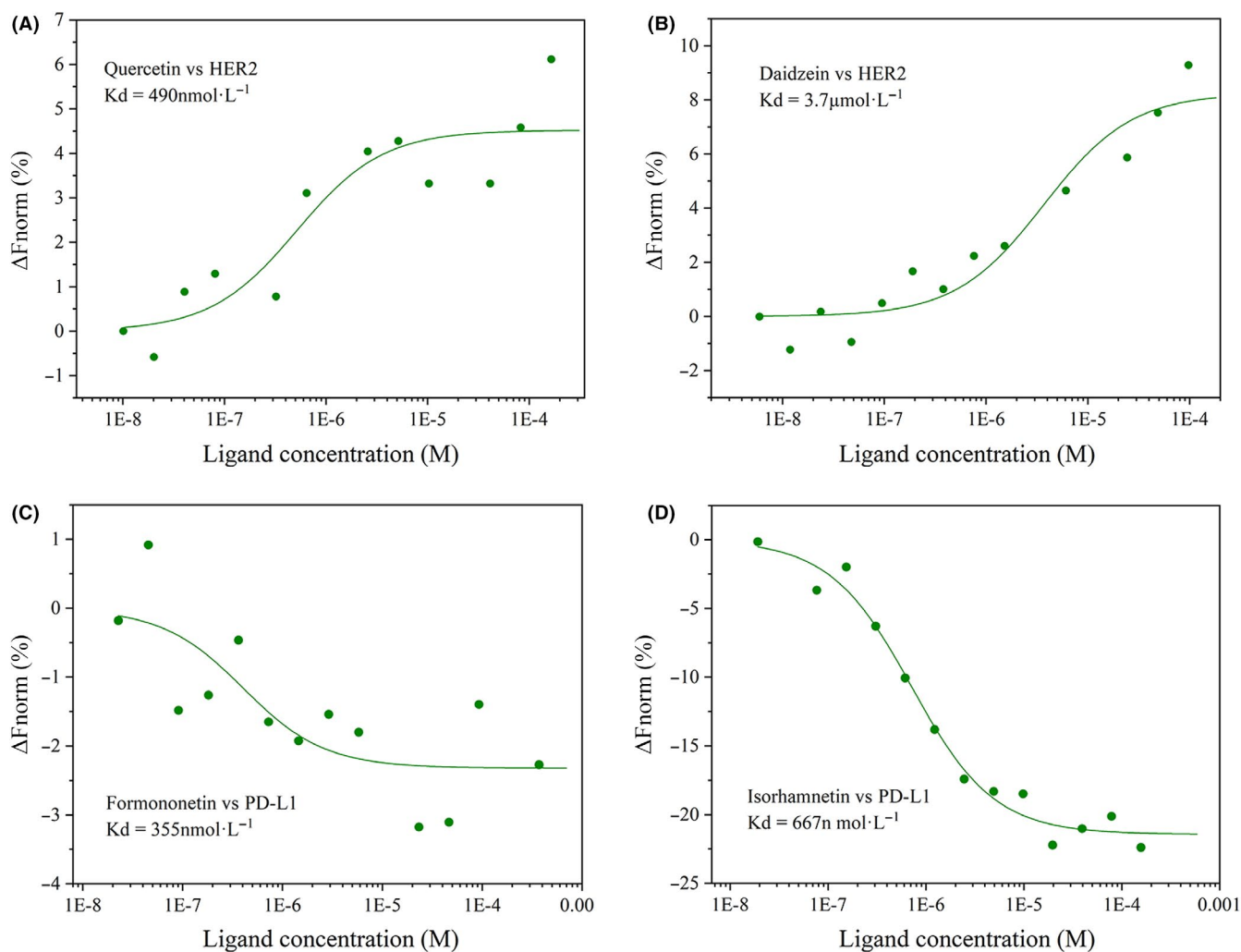
FIGURE 3 Results of microscale thermophoresis. A, Quercetin vs human epidermal growth factor receptor 2 (HER2). B, Daidzein vs HER2. C, Formononetin vs programmed cell death 1-ligand 1 (PD-L1). D, Isorhamnetin vs PD-L1
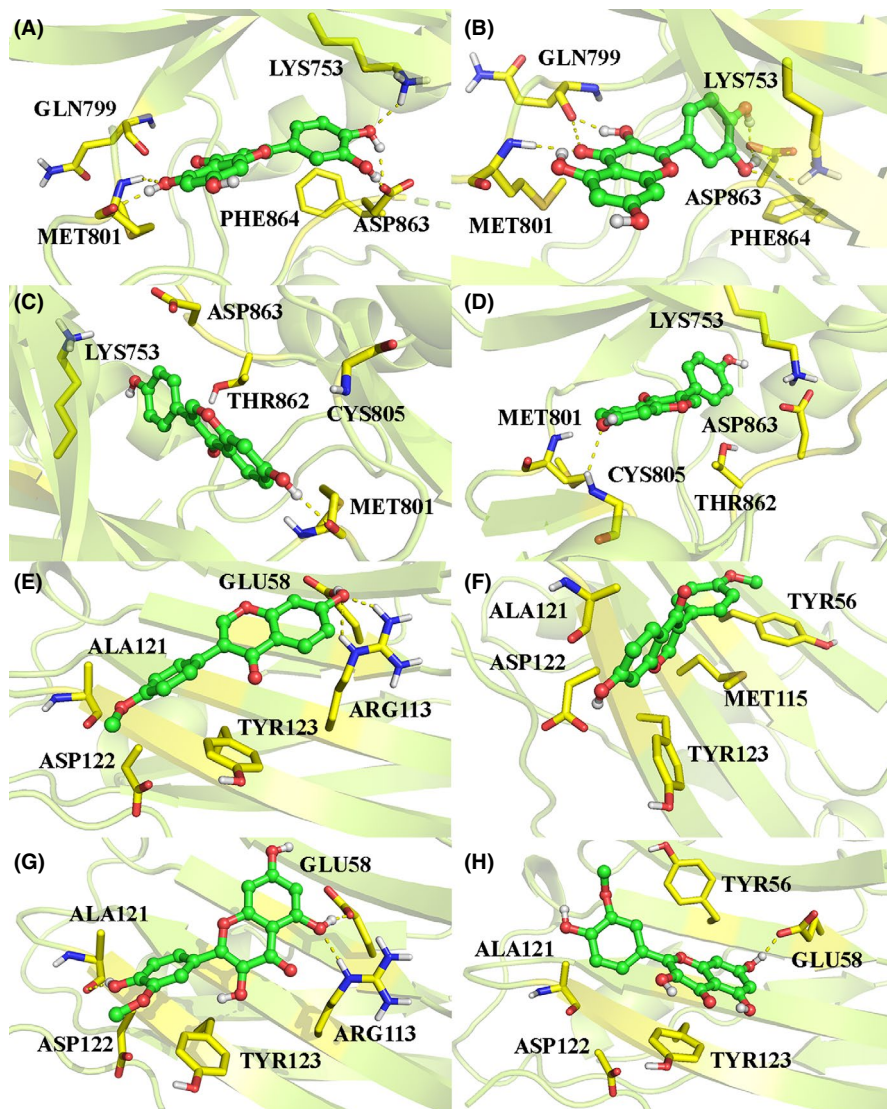
FIGURE 4 Interaction mode of compounds with the target proteins. A, Quercetin vs human epidermal growth factor receptor 2 (HER2) before molecular dynamics simulation (MD). B, Quercetin vs HER2 after MD. C, Daidzein vs HER2 before MD. D, Daidzein vs HER2 after MD. E, Formononetin vs programmed cell death 1-ligand 1 (PD-L1) before MD. F, Formononetin vs PD-L1 after MD. G, Isorhamnetin vs PD-L1 before MD. H, Isorhamnetin vs PD-L1 after MD

pocket is necessary to achieve better binding. The chromone moiety of formononetin is closer to Ala121, Asp122, and Tyr123 after a 50 ns MD (Figure 4H). Both MM-PBSA and MST showed that formononetin had higher binding free energy and affinity with PD-L1, indicating that formononetin can achieve a better binding pattern by conformational adjustment. The pocket is made up of Glu58, Arg113, Ala121, Asp122, and Tyr123, which are key residues blocking PD-1/PD-L1 interaction.[30,53] Zak et al[54] reported that BMS-202 and BMS-8, as PD-1/PD-L1 blockers, could interact with PD-L1 Ala121, Asp122, and Tyr123.

By conformational analysis, in summary, quercetin and formononetin are two key compounds in GQBZP and have strong ability to target HER2 and PD-L1 with ideal modes of action.

Binding free energies between compounds and proteins were calculated by the MM-PBSA method after MST, and the results are shown in Table 6. The binding free energies of quercetin and daidzein with HER2 are −26.55 kcal/mol and −14.18 kcal/mol, respectively, and the binding free energies of formononetin and isorhamnetin with PD-L1 are −19.41 kcal/mol and −11.86 kcal/mol, respectively, which is consistent with the MST assays.

TABLE 6 Binding free energies and energy components calculated by the molecular mechanics Poisson-Boltzmann surface area method (kcal/mol)

	Quercetin	Daidzein	Formononetin	Isorhamnetin
HER2	−26.55	−14.18	no data	no data
PD-L1	no data	no data	−19.41	−11.86

HER2, human epidermal growth factor receptor 2; PD-L1, programmed cell death 1-ligand 1.

3.4 | Compounds targeting HER2 and PD-L1 suppressed cell proliferation

Although we have confirmed that the compounds have high affinity with the target proteins, whether they have inhibitory effects still needs verification. We measured the effect of these compounds on the proliferation of GC cells. First, we used western blot to detect the expression of HER2 and PD-L1 in the MKN-45, SGC-7901,

and BGC-823 GC cell lines and gastric mucosal epithelial GES-1 cell line. The results showed that HER2 and PD-L1 are highly expressed in MKN-45 cells (Figure 5A,B). We used confocal microscopy to verify this result, which is consistent with western blot analysis (Figure 5C,D).

As we had confirmed that HER2 and PD-L1 were overexpressed in MKN-45 cells, the cytotoxic activities of compounds targeting HER2 and PD-L1[55] were determined by CCK-8 assay; the IC_{50} values of quercetin, daidzein, and isorhamnetin were 19.27 μmol/L, 21.48 μmol/L, and 10.84 μmol/L, respectively. Formononetin could not inhibit proliferation of tumor cells, as shown in Figure 6. Studies

have shown that formononetin can block the activation and translocation of nuclear factor - kappa beta (NF-kB) in INS-1 cells induced by IL-1β. It has a good antiinflammatory effect, which could also include immunoregulation through this pathway.[56] Formononetin and some of its metabolites could play an immunoregulatory role by enhancing the production of IL-4 in T cells.[57] Wang et al[58] found that isorhamnetin can enhance innate immunity by interfering in an immune-damaged mouse model. Shi et al[59] also found that isorhamnetin can prevent or treat chronic inflammation, autoimmune diseases, and transplant rejection by regulating the role of cytokines in dendritic cells.[60] This group found that isorhamnetin and
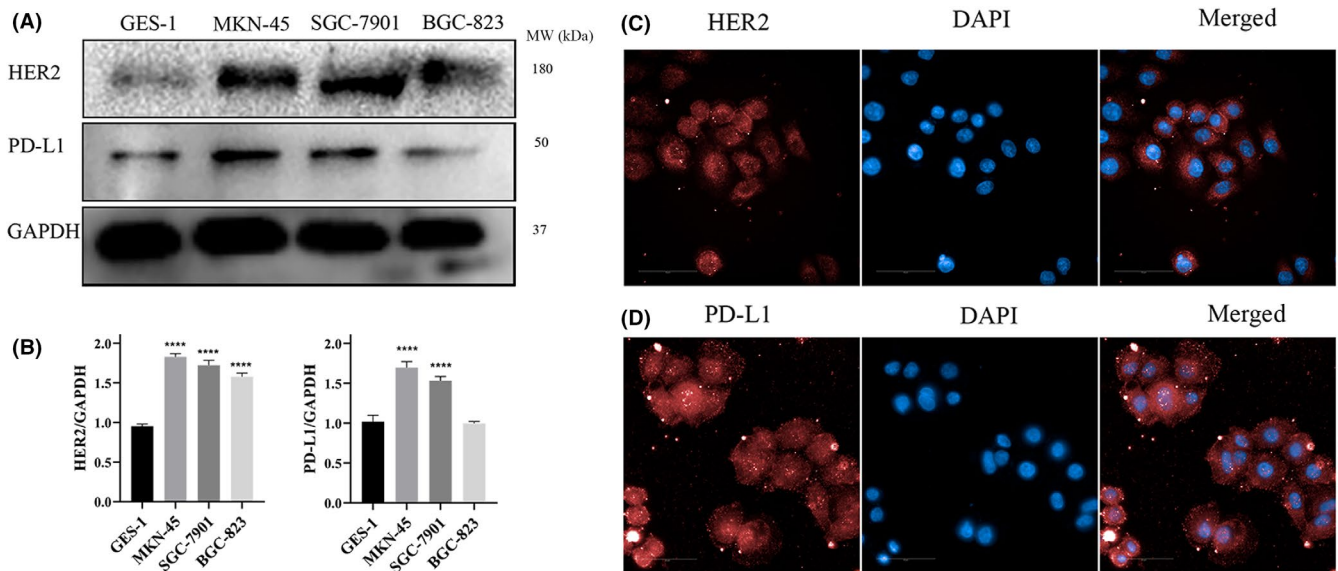
FIGURE 5 Screening results of cell lines expressing human epidermal growth factor receptor 2 (HER2) and programmed cell death 1-ligand 1 (PD-L1). A, Western blot analysis of HER2 and PD-L1 in MKN-45, SGC-7901, BGC-823, and GES-1 cells. B, Relative HER2 and PD-L1 expression levels were quantified by normalization to GAPDH. ns, not significant. ****P <.0001. C, D, Images of HER2 and PD-L1 immunofluorescence in MKN-45 cells. Scale bar = 50 μm
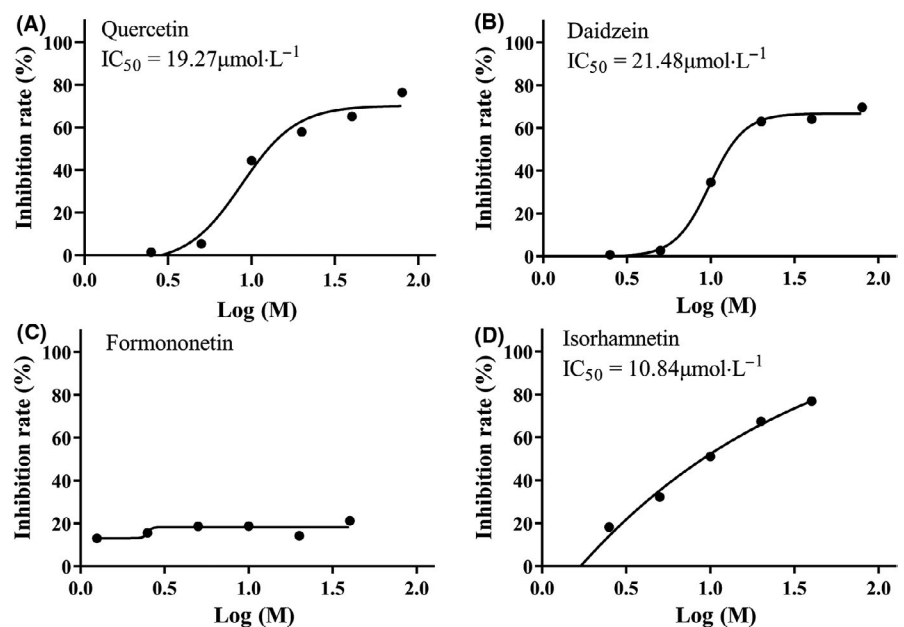
FIGURE 6 Inhibitory effects of compounds on MKN-45 cell. A, Quercetin. B, Daidzein. C, Formononetin, D, Isorhamnetin

formononetin, the active ingredients in *Astragali radix*, have immunoregulatory effects, through the study of network pharmacology. Our cell experiments yielded different results, however, which warrants further exploration.

3.5 | Quercetin suppressed HER2 kinase

According to the molecular docking analysis and cell proliferation assays, target prediction suggested that quercetin might be a potential HER2 kinase inhibitor. To verify this and explore the mechanisms of the compounds, the inhibitory effects of quercetin against the HER2 kinase were determined. The results show that quercetin strongly suppresses HER2 kinases, with an IC_{50} value of 570.07 nmol/L, as shown in Figure 7.

Quercetin impedes the propagation of various types of cancers, such as lung, prostate, liver, breast, colon, and cervical cancer.[61] Quercetin functions through various mechanisms involved in cell signaling and has the ability to inhibit carcinogen-activating enzymes, showing anticancer effects based on binding to cell receptors and proteins.[62,63] Furthermore, quercetin has been recently reported to have synergistic effects when combined with chemotherapeutic agents such as cisplatin, which could further improve the outcomes of traditional chemotherapy.[64] Although compared with a positive drug, the docking scores and affinity of compounds of TCM with target protein (HER2) might be lower, the probability of drug resistance to those compounds might also be lower, and compared with mAbs, these compounds have the advantages of short half-life, minimal side-effects, and low cost.[65] In addition, quercetin can cooperate with multiple compounds to avoid the adverse effects of strong binding of a single molecule. At the same time, quercetin can be used as a skeleton to modify its structure, or on this basis to screen other compounds of TCM based on structure matching. Moreover, the results of quercetin derivatives reported from 2012 to 2016 revealed that quercetin derivatives had higher biological activity, including

higher cytotoxicity to breast cancer cells, HeLa cells, HepG2 cells, and other cells, than quercetin.[66]

The therapeutic effect of compounds of TCM might not be better than that of mAbs, but they have the advantages of high oral bioavailability and few side-effects, and so have great prospects for clinical development. Quercetin and formononetin in GQBZP have stronger affinity for HER2 and PD-L1, respectively, and could be the key compounds in the prescriptions for two-way treatment of cancer by inhibiting the proliferation of cancer cells and improving the immune function of the body.

4 | DISCUSSION

Traditional Chinese medicine is a comprehensive medicinal system, which has potential utilization based on thousands of years in clinical practice in China, providing the characteristics of multi-components and multitargets and presenting a potent synergistic effect for treatment of various diseases with fewer side-effects.[67] The effectiveness of TCM in treating diseases has been recognized worldwide,[68-70] but the material basis, potential mechanisms, interaction relationships, and modes of action of TCM and possible targets are still unclear, which limits the precise use and modern development of TCM. The above results show that, although our results do not have higher docking scores and binding affinities than those of approved mAbs or small molecule inhibitors, we preliminarily verify the theory of "synergistic pharmacological effect with multicomponents and multitargets" of TCM using network pharmacology, multitarget molecular docking, molecular dynamics simulation, and protein and cell experiments in vitro, and explain the possible material basis of GQBZP in the treatment of GC. Moreover, the clinical use of TCM can benefit from the synergistic effects of the ingredients, reduce adverse reactions, and effects of single drug treatment, and has better clinical application value. However, this study is limited to in vitro experiments and it is still necessary to further explore the potential activity of the active compounds of GQBZP with experimental studies in vivo to reveal the molecular mechanisms of its clinical therapeutic effect on GC. We are committed to establishing a systematic research method based on network pharmacology, multitarget molecular docking, molecular dynamics simulation, and protein and experimental verification in vitro and in vivo, to establish a systematic analysis method for TCM treatment of diseases, so as to provide a possible theoretical and experimental basis for the standardization and internationalization of TCM.
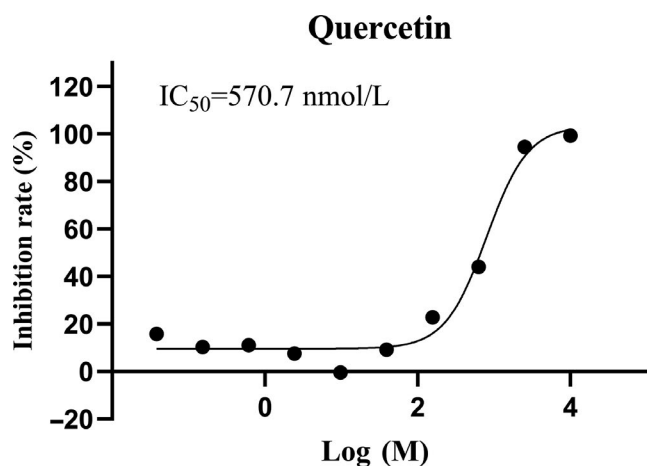
FIGURE 7 Enzyme inhibitory activity of human epidermal growth factor receptor 2

CONFLICT OF INTEREST

The authors have no conflict of interest.

ORCID

Ling Li https://orcid.org/0000-0002-9349-8332

REFERENCES

1. Verma R, Sharma PC. Next generation sequencing-based emerging trends in molecular biology of gastric cancer. *Am J Cancer Res*. 2018;8:207-225.
2. Lim B, Kim JH, Kim M, Kim SY. Genomic and epigenomic heterogeneity in molecular subtypes of gastric cancer. *World J Gastroenterol*. 2016;22:1190-1201.
3. Roviello G, D'Angelo A, Generali D, et al. Avelumab in gastric cancer. *Immunotherapy*. 2019;11:759-768.
4. Jin H, Li P, Mao C, et al. Pathological complete response after a single dose of Anti-PD-1 therapy in combination with chemotherapy as a first-line setting in an unresectable locally advanced gastric cancer with PD-L1 positive and microsatellite instability. *Onco Targets Ther*. 2020;13:1751-1756.
5. Bang YJ, Van Cutsem E, Feyereislova A, et al. Trastuzumab in combination with chemotherapy versus chemotherapy alone for treatment of HER2-positive advanced gastric or gastro-oesophageal junction cancer (ToGA): a phase 3, open-label, randomised controlled trial. *Lancet*. 2010;376:687-697.
6. Chaganty BKR, Qiu S, Gest A, et al. Trastuzumab upregulates PD-L1 as a potential mechanism of trastuzumab resistance through engagement of immune effector cells and stimulation of IFNγ secretion. *Cancer Letters*. 2018;430:47-56.
7. Hopkins AL. Network pharmacology: the next paradigm in drug discovery. *Nat Chem Biol*. 2008;4:682-690.
8. Zhu Di. *Prescriptions for Universal Relief*. Vol. 7. Beijing: People's Health Publishing House; 1983.
9. Li-xin ZHANG, Lei WANG, Yi-ming ZHANG, et al. Protective effect of GuiQi Baizhu Recipe on hepatotoxicity induced by cisplatin in mice. *Chin J Clin Pharmacol*. 2019;35:788-790,794.
10. Lei WANG, Xiao-min XU, Yan-hui ZHANG, et al. Attenuation effect of Guiqi Baizhu prescription on renal injury induced by cisplatin. *Chin J Clin Pharmacol*. 2018;43:917-923.
11. Ling LI, Feng-mei WANG, Yong-qi LIU, et al. Clinical trial of the auxiliary treatment with Gui Qi Bai Zhu fang in the treatment of patients with gastric cancer. *Chin J Clin Pharmacol*. 2017;33:1184-1187.
12. Zhang X, Wang D, Ren X, Atanasov AG, Zeng R, Huang L. System bioinformatic approach through molecular docking, network pharmacology and microarray data analysis to determine the molecular mechanism underlying the effects of rehmanniae Radix praeparata on cardiovascular diseases. *Curr Protein Pept Sci*. 2019;20:964-975.
13. Tao Q, Du J, Li X, et al. Network pharmacology and molecular docking analysis on molecular targets and mechanisms of Huashi Baidu formula in the treatment of COVID-19. *Drug Dev Ind Pharm*. 2020;46:1345-1353.
14. Zhou C, Liu L, Zhuang J, et al. A systems biology-based approach to uncovering molecular mechanisms underlying effects of traditional Chinese medicine Qingdai in chronic myelogenous leukemia, involving integration of network pharmacology and molecular docking technology. *Med Sci Monit*. 2018;24:4305-4316.
15. Guo W, Huang J, Wang N, et al. Integrating network pharmacology and pharmacological evaluation for deciphering the action mechanism of herbal formula Zuojin Pill in suppressing hepatocellular carcinoma. *Front Pharmacol*. 2019;10:1185.
16. Li J, Ma X, Liu C, et al. Exploring the mechanism of Danshen against Myelofibrosis by network pharmacology and molecular docking. *Evid Based Complement Alternat Med*. 2018;2018:8363295.
17. Grinter SZ, Zou X. Challenges, applications, and recent advances of protein-ligand docking in structure-based drug design. *Molecules*. 2014;19:10150-10176.
18. Wang C, Greene D, Xiao L, Qi R, Luo R. Recent developments and applications of the MMPBSA method. *Front Mol Biosci*. 2017;4:87.
19. Seidel SA, Dijkman PM, Lea WA, et al. Microscale thermophoresis quantifies biomolecular interactions under previously challenging conditions. *Methods*. 2013;59:301-315.
20. Ru J, Li P, Wang J, et al. TCMSP: a database of systems pharmacology for drug discovery from herbal medicines. *J Cheminformatics*. 2014;6:13.
21. Kim S, Chen J, Cheng T, et al. PubChem 2019 update: improved access to chemical data. *Nucleic Acids Res*. 2019;47:D1102-D1109.
22. Gfeller D, Grosdidier A, Wirth M, Daina A, Michielin O, Zoete V. SwissTargetPrediction: a web server for target prediction of bioactive small molecules. *Nucleic Acids Res*. 2014;42:W32-W38.
23. Chen X, Ji ZL, Chen YZTTD. Therapeutic target database. *Nucleic Acids Res*. 2002;30:412-415.
24. Wishart DS, Feunang YD, Guo AC, et al. DrugBank 5.0: a major update to the DrugBank database for 2018. *Nucleic Acids Res*. 2018;46:D1074-d1082.
25. Lopes CT, Franz M, Kazi F, Donaldson SL, Morris Q, Bader GD. Cytoscape Web: an interactive web-based network browser. *Bioinformatics*. 2010;26:2347-2348.
26. Huang DW, Sherman BT, Lempicki RA. Systematic and integrative analysis of large gene lists using DAVID bioinformatics resources. *Nat Protoc*. 2009;4:44-57.
27. Wang X, Su R, Guo Q, Liu J, Ruan B, Wang G. Competing endogenous RNA (ceRNA) hypothetic model based on comprehensive analysis of long non-coding RNA expression in lung adenocarcinoma. *PeerJ*. 2019;7:e8024.
28. Franceschini A, Szklarczyk D, Frankild S, et al. STRING v9.1: protein-protein interaction networks, with increased coverage and integration. *Nucleic Acids Res*. 2013;41:D808-815.
29. Santos GB, Ganesan A, Emery FS. Oral administration of peptide-based drugs: beyond Lipinski's Rule. *ChemMedChem*. 2016;11:2245-2251.
30. Ishikawa T, Seto M, Banno H, et al. Design and synthesis of novel human epidermal growth factor receptor 2 (HER2)/epidermal growth factor receptor (EGFR) dual inhibitors bearing a pyrrolo[3,2-d]pyrimidine scaffold. *J Med Chem*. 2011;54:8030-8050.
31. Zak KM, Kitel R, Przetocka S, et al. Structure of the complex of human programmed death 1, PD-1, and its ligand PD-L1. *Structure*. 1993;2015(23):2341-2348.
32. Berman HM, Westbrook J, Feng Z, et al. The protein data bank. *Nucleic Acids Res*. 2000;28:235-242.
33. Sheikh IA, Jiffri EH, Ashraf GM, Kamal MA, Beg MA. Structural studies on inhibitory mechanisms of antibiotic, corticosteroid and catecholamine molecules on lactoperoxidase. *Life Sci*. 2018;207:412-419.
34. Friesner RA, Murphy RB, Repasky MP, et al. Extra precision glide: docking and scoring incorporating a model of hydrophobic enclosure for protein-ligand complexes. *J Med Chem*. 2006;49:6177-6196.
35. Friesner RA, Banks JL, Murphy RB, et al. Glide: a new approach for rapid, accurate docking and scoring. 1. Method and assessment of docking accuracy. *J Med Chem*. 2004;47:1739-1749.
36. Manchester J, Walkup G, Rivin O, You Z. Evaluation of pKa estimation methods on 211 druglike compounds. *J Chem Inf Model*. 2010;50:565-571.
37. Yuan S, Chan HCS, Filipek S, Vogel H. PyMOL and inkscape bridge the data and the data visualization. *Structure*. 1993;2016(24):2041-2042.

38. Wang J, Wolf RM, Caldwell JW, Kollman PA, Case DA. Development and testing of a general amber force field. *J Comput Chem*. 2004;25:1157-1174.

39. Cerutti DS, Duke RE, Darden TA, Lybrand TP. Staggered mesh Ewald: an extension of the smooth particle-mesh Ewald method adding great versatility. *J Chem Theory Comput*. 2009;5:2322.

40. Lee TS, Allen BK, Giese TJ, et al. Alchemical binding free energy calculations in Amber20: advances and best practices for drug discovery. *J Chem Inf Model*. 2020;60:5595-5623.

41. Eslami H, Mojahedi F, Moghadasi J. Molecular dynamics simulation with weak coupling to heat and material baths. *J Chem Phys*. 2010;133:084105.

42. Kollman PA, Massova I, Reyes C, et al. Calculating structures and free energies of complex molecules: combining molecular mechanics and continuum models. *Acc Chem Res*. 2000;33:889-897.

43. Lan Y, Wang Y, Huang K, Zeng Q. Heat shock protein 22 attenuates doxorubicin-induced cardiotoxicity via regulating inflammation and apoptosis. *Front Pharmacol*. 2020;11:257.

44. Yao D, Pan D, Zhen Y, et al. Ferulin C triggers potent PAK1 and p21-mediated anti-tumor effects in breast cancer by inhibiting Tubulin polymerization in vitro and in vivo. *Pharmacol Res*. 2020;152:104605.

45. Liberelle M, Magnez R, Thuru X, et al. MUC4-ErbB2 oncogenic complex: binding studies using microscale thermophoresis. *Sci Rep*. 2019;9:16678.

46. Mascia F, Schloemann DT, Cataisson C, et al. Cell autonomous or systemic EGFR blockade alters the immune-environment in squamous cell carcinomas. *Int J Cancer*. 2016;139:2593-2597.

47. Suh KJ, Sung JH, Kim JW, et al. EGFR or HER2 inhibition modulates the tumor microenvironment by suppression of PD-L1 and cytokines release. *Oncotarget*. 2017;8:63901–63910.

48. Atkins MB, Larkin J. Immunotherapy combined or sequenced with targeted therapy in the treatment of solid tumors: current perspectives. *J Natl Cancer Inst*. 2016;108:djv414.

49. Tang J, Yu JX, Hubbard-Lucey VM, Neftelinov ST, Hodge JP, Lin Y. Trial watch: the clinical trial landscape for PD1/PDL1 immune checkpoint inhibitors. *Nat Rev Drug Discovery*. 2018;17:854-855.

50. Yong W, Chun LI, Qi Q, et al. Study of collaborative evaluation system on synergistic pharmacological effect of chinese formula with multi-components and multi-targets. *Sci Sin Vitae*. 2016;46:1029-1032.

51. Elkamhawy A, Farag AK, Viswanath AN, et al. Targeting EGFR/HER2 tyrosine kinases with a new potent series of 6-substituted 4-anilinoquinazoline hybrids: Design, synthesis, kinase assay, cell-based assay, and molecular docking. *Bioorg Med Chem Lett*. 2015;25:5147-5154.

52. Li J, Wang H, Li J, Bao J, Wu C. Discovery of a potential HER2 inhibitor from natural products for the treatment of HER2-positive breast cancer. *Int J Mol Sci*. 2016;17(7):1055

53. Magiera-Mularz K, Skalniak L, Zak KM, et al. Bioactive macrocyclic inhibitors of the PD-1/PD-L1 immune checkpoint. *Angew Chem Int Ed Engl*. 2017;56:13732-13735.

54. Zak KM, Grudnik P, Magiera K, Dömling A, Dubin G, Holak TA. Structural biology of the immune checkpoint receptor PD-1 and its ligands PD-L1/PD-L2. *Structure*. 2017;25:1163-1174.

55. Ashizawa T, Iizuka A, Tanaka E, et al. Antitumor activity of the PD-1/PD-L1 binding inhibitor BMS-202 in the humanized MHC-double knockout NOG mouse. *Biomed Res*. 2019;40:243-250.

56. Huang GC, Lee CJ, Wang KT, et al. Immunomodulatory effects of *Hedysarum polybotrys* extract in mice macrophages, splenocytes and leucopenia. *Molecules*. 2013;18:14862-14875.

57. Park J, Kim SH, Cho D, Kim TS. Formononetin, a phyto-oestrogen, and its metabolites up-regulate interleukin-4 production in activated T cells via increased AP-1 DNA binding activity. *Immunology*. 2005;116:71-81.

58. Wang H, Zhang Q, Cheng ML, et al. Effect of the Miaoyao Fanggan sachet-derived isorhamnetin on TLR2/4 and NKp46 expression in mice. *J Ethnopharmacol*. 2012;144:138-144.

59. Shi H, He J, Li X, et al. Isorhamnetin, the active constituent of a Chinese herb Hippophae rhamnoides L, is a potent suppressor of dendritic-cell maturation and trafficking. *Int Immunopharmacol*. 2018;55:216-222.

60. Liu J, Nile SH, Xu G, Wang Y, Kai G. Systematic exploration of *Astragalus membranaceus* and Panax ginseng as immune regulators: Insights from the comparative biological and computational analysis. *Phytomedicine*. 2019;153077.

61. Rauf A, Imran M, Khan IA, et al. Anticancer potential of quercetin: a comprehensive review. *Phytother Res*. 2018;32:2109-2130.

62. Shih H, Pickwell GV, Quattrochi LC. Differential effects of flavonoid compounds on tumor promoter-induced activation of the human CYP1A2 enhancer. *Arch Biochem Biophys*. 2000;373:287-294.

63. Murakami A, Ashida H, Terao J. Multitargeted cancer prevention by quercetin. *Cancer Lett*. 2008;269:315-325.

64. Brito AF, Ribeiro M, Abrantes AM, et al. Quercetin in cancer treatment, alone or in combination with conventional therapeutics? *Curr Med Chem*. 2015;22:3025-3039.

65. Cheng B, Yuan WE, Su J, Liu Y, Chen J. Recent advances in small molecule based cancer immunotherapy. *Eur J Med Chem*. 2018;157:582-598.

66. Massi A, Bortolini O, Ragno D, et al. Research progress in the modification of quercetin leading to anticancer agents. *Molecules*. 2017;22:1270.

67. Ma S, Feng C, Zhang X, et al. The multi-target capabilities of the compounds in a TCM used to treat sepsis and their in silico pharmacology. *Complement Ther Med*. 2013;21:35-41.

68. Yang W, Li MQ, Li Y, et al. [Exploring Chinese medicine and Western medicine group modules in acute phase of ischemic stroke disease]. Zhongguo Zhong yao za zhi = Zhongguo zhongyao zazhi =. *China J Chin Materia Med*. 2018;43:618-626.

69. Zhang HY, Wang HL, Zhong GY, Zhu JX. Molecular mechanism and research progress on pharmacology of traditional Chinese medicine in liver injury. *Pharmaceut Biol*. 2018;56:594-611.

70. Zhang J, Meng H, Zhang Y, et al. The therapeutic effect of Chinese medicine for the treatment of atherosclerotic coronary heart disease. *Curr Pharm Des*. 2017;23:5086-5096.

SUPPORTING INFORMATION

Additional supporting information may be found online in the Supporting Information section.